Electroanalysis

DOI: 10.1002/ange.200601640

Thermodynamic and Kinetic Enhancement of Electrochemical Sensitivity by Chemical Coupling in Microfluidic Systems**

*Imtiaz M. Khalid, Qiaosheng Pu, and Julio C. Alvarez**

Herein, we report the enhancement of electrochemical sensitivity by chemical coupling of two independent reactions in a microfluidic channel. Scheme 1 illustrates the general concept of this approach: an upstream electrode (E_1) drives a reaction that produces protons while a downstream electrode (E_2) conducts a second reaction that consumes protons. The reactions are chemically coupled by the electrogenerated protons, which are used to harness thermodynamically or kinetically the reaction at E_2. Herein, we show two examples of a positive shift in the redox potential ($E^{\circ\prime}$) of an analyte in

[*] I. M. Khalid, Dr. Q. Pu, Prof. J. C. Alvarez
Department of Chemistry
Virginia Commonwealth University
Richmond, VA, 23284–2006 (USA)
Fax: (+1) 804-828-8599
E-mail: jcalvarez2@vcu.edu

[**] This work is supported by Virginia Commonwealth University and the Jeffress Memorial Trust of Virginia.

Supporting information for this article is available on the WWW under http://www.angewandte.org or from the author.

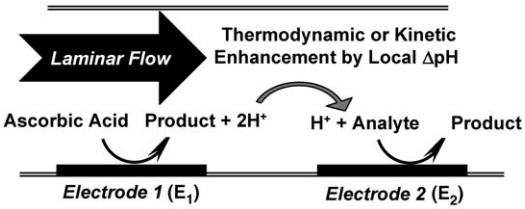

Scheme 1. Chemical coupling of electrochemical reactions.

response to electrogeneration of protons at E_1. As a result of this shift, two effects with analytical value arise: first, the analyte is now fully detectable at potentials more positive than $E^{\circ\prime}$, where the analyte is undetectable; and second, two redox analytes with overlapping $E^{\circ\prime}$ values can be discriminated if one of them is not sensitive to protonation. The most significant aspect of this approach is that the effects reported herein are observable as a result of using a microfluidic cell instead of a traditional electrochemical cell. Prior work in the area of hydrodynamic voltammetry[1–7] and the generation of chemical gradients in flow systems is directly related to the present work.[8–12]

The advantage of chemically coupled reactions as depicted in Scheme 1 can be realized by considering a biochemical process such as the conversion of phospho-(enol)pyruvate (PEP) into pyruvate in the glycolisis cycle.[13] The phosphorylation of adenosine diphosphate (ADP) to form adenosine triphosphate (ATP) is an energetically unfavorable process. However, when this reaction is coupled to the exergonic hydrolysis of PEP that produces pyruvate and inorganic phosphate, the net reaction becomes energetically favorable with an overall negative ΔG°.[13] We used this principle to enhance the current response for the reduction of model analytes [Eq. (1)] by using the oxidation of ascorbic

$$\mathrm{DMBQ} + 2\,\mathrm{H^+} + 2\,\mathrm{e^-} \rightarrow \mathrm{H_2DMBQ} \qquad \Delta G^{\circ\prime} = +42.8\ \mathrm{kJ\,mol^{-1}}\ (\mathrm{pH}\ 7.0) \tag{1}$$

acid (AA) that produces dehydroascorbic acid (DAA) and protons [Eq. (2)].[14] The only requirement to observe the

$$\mathrm{AA} \rightarrow \mathrm{DAA} + 2\,\mathrm{H^+} + 2\,\mathrm{e^-} \quad \Delta G^{\circ\prime} = -57.1\ \mathrm{kJ\,mol^{-1}}\ (\mathrm{pH}\ 7.0) \tag{2}$$

effect is that the analyte reaction must involve the consumption of protons so that the overall $\Delta G^{\circ\prime}$ value [Eq. (3)] can be made more negative than that of the analyte reaction alone.

$$\mathrm{AA} + \mathrm{DMBQ} \rightarrow \mathrm{H_2DMBQ} + \mathrm{DAA} \qquad \text{Total } \Delta G^{\circ\prime} = -14.3\ \mathrm{kJ\,mol^{-1}} \tag{3}$$

Figure 1 shows the reduction of dimethyl benzoquinone (DMBQ) at two different pH values under buffer conditions. An overall decrease of 4.4 units in pH produced a positive shift in $E^{\circ\prime}$ from −0.310 to −0.089 V,[15] which translates into an average of around 50.3 mV/pH unit, which is similar to the shift observed for other quinones.[16] Figure 2 shows a series of data points obtained for coupling experiments in nonbuffered solution mixtures of AA and DMBQ with the initial pH adjusted to 7.0. The reduction of DMBQ was monitored at E_2 while the potential of E_1 (and hence rate of oxidation of AA)

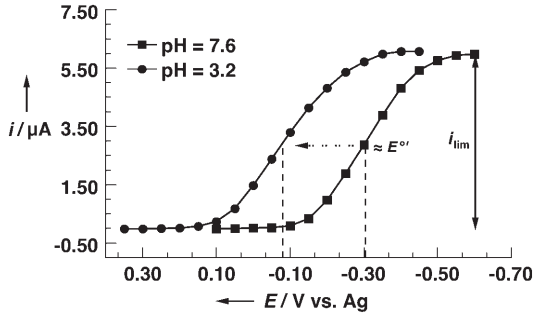

Figure 1. Voltammetry of 5.0 mM DMBQ in a microfluidic channel with 0.1 M phosphate buffer and 0.1 M KCl.

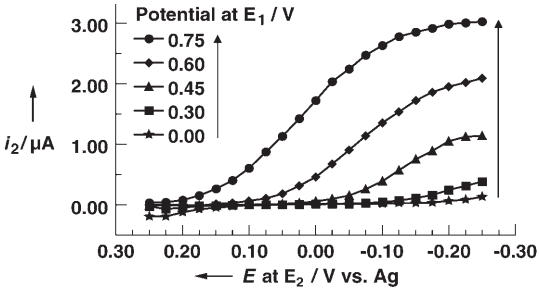

Figure 2. Voltammetry under coupling conditions of 5.0 mM DMBQ, 10 mM AA, and 0.1 M KCl; initial pH = 7.0 (no buffer).

was increased; no oxidation of AA was observed at 0.00 V and a maximum rate was observed at 0.75 V (see the Supporting Information). As the oxidation of AA is a two-electron process that generates two protons and the electroinactive species DAA,[14] AA can not be redox recycled at E_2.

The production of protons at E_1 induces an increase of the current at E_2 in a potential window in which quinone is not reduced at neutral pH (Figure 1). At the maximum rate of proton production on E_1 (0.75 V), the final $E^{\circ\prime}$ value observed for the quinone was 0.016 V with an overall positive shift of 0.422 V. A similar trend with somewhat diminished shift was observed when the experiment was conducted under buffered conditions at pH 7.0 (see the Supporting Information). Table 1 summarizes the $E^{\circ\prime}$ and limiting current i_{lim} values at different buffer concentrations. The $E^{\circ\prime}$ value obtained for DMBQ under coupling conditions was always less positive as the ionic strength of the buffer increased. Likewise, the i_{lim} values for the reduction of DMBQ in 1.0 M buffer was about 50% lower than that obtained in 0.05 M buffer.

To verify the local pH decrease upon AA oxidation, we monitored this reaction in the presence of a pH indicator with a fluorescence microscope.[17,18] The fluorescence of the dye

Table 1: Effect of buffer strength on $E^{\circ\prime}$ DMBQ at E_2.

Buffer concentration [M][a]	$E^{\circ\prime}$ [V][b]	i_{lim} [μA]
0.05	−0.087	4.24
0.10	−0.106	4.06
0.50	−0.158	3.10
1.0	−0.172	2.31

[a] pH 7.0. [b] E_1 kept at 0.75 V.

was negligible at the initial pH 7.0 (see the Supporting Information), but there was a local increase in fluorescence around the transparent electrode after the electrode potential was stepped to 0.900 V for 3 s (Figure 3).

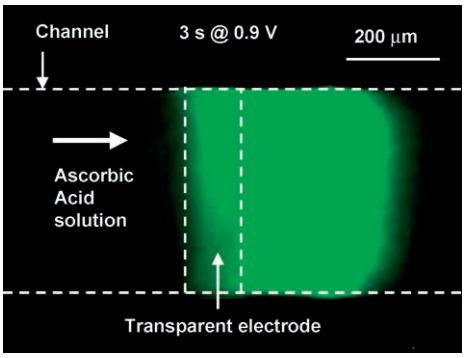

Figure 3. Fluorescence monitoring of proton release upon electrooxidation of 36 mM AA and 0.1 M NaCl with an initial pH of 7.0 and 10 μM Lyzosensor DND-160; excitation wavelength = 365 nm, emission wavelength > 515 nm.

The effect of the protons on DMBQ can be understood by considering Equation (1) and the coupling principle described above. We detected a redox wave about 0.3 V more positive than the quinone reduction wave when HCl was added to pure DMBQ (see the Supporting Information). The same wave was observed for mixtures of AA and DMBQ when the voltammetric scan included the oxidation of AA. These results are consistent with previous reports[15] and support the presence of an intermediate that is stabilized by protonation and is responsible for the positive thermodynamic shifts observed above.

To illustrate how the proton coupling enhances the detection sensitivity for DMBQ in a microfluidic cell, we performed calibration curves with mixtures of AA and DMBQ at different concentrations of DMBQ. Figure 4 shows a series of data points obtained under three different conditions: a mixture AA and DMBQ with proton coupling (A); the same mixture measured without proton coupling (B); and a pure DMBQ solution under the conditions of proton coupling (C). The slope of the fitted line for data set A

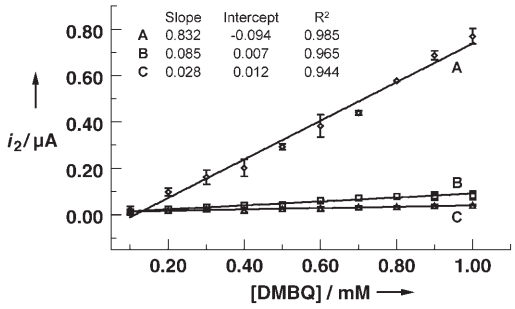

Figure 4. Calibration curve for a 1:4 mixture of DMBQ and AA in 0.1 M KCl; initial pH = 7.3, E_1 was kept at 0.750 V while E_2 was pulsed at −0.225 V vs. Ag. A) DMBQ coupled signal; B, C) controls (see text).

is about 10 times higher than that for the control experiment B and approximately 30 times that for C.

The reduction of $[Ru(NH_3)_6]^{3+}$ [Eq. (4)] at E_2 was investigated because the ammonia ligand is basic. However, the

$$[Ru(NH_3)_6]^{3+} + e^- \rightarrow [Ru(NH_3)_6]^{2+}\ (E_2) \qquad (4)$$

ligand exchange kinetics of $[Ru(NH_3)_6]^{3+}$ is so slow[19] relative to the time scale of conventional voltammetric experiments that in neutral or weakly acidic conditions the voltammetry of $[Ru(NH_3)_6]^{3+}$ appears relatively insensitive to pH. Taube and co-workers[19] found that the slow aquation rate for $[Ru(NH_3)_6]^{2+}$ [Eq. (5), $k \approx 1.24 \times 10^{-3}\,M^{-1}s^{-1}$] can be accelerated significantly in acidic conditions.[19]

$$H_2O + [Ru(NH_3)_6]^{2+} + H^+ \rightarrow [Ru(NH_3)_5H_2O]^{2+} + NH_4^+ \qquad (5)$$

Since Equation (5) involves the product of Equation (4), the addition of protons promotes Equation (4) with a concomitant positive shift in $E^{\circ\prime}$. Figure 5 shows the effect

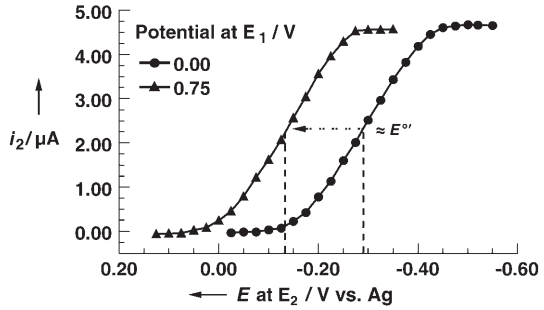

Figure 5. Voltammetry under coupling conditions for 5.0 mM $[Ru(NH_3)_6]^{3+}$, 4.0 mM AA, and 0.1 M KCl; initial pH 3.1 (no buffer).

of changing the potential of E_1 from 0.00 to 0.75 V while reducing $[Ru(NH_3)_6]^{3+}$ at E_2 in a solution mixture with AA initially at pH 3.1. A positive shift from −0.293 to −0.137 V was observed when E_1 was set to obtain the maximum rate of proton generation. Although the overall effect is thermodynamic, we consider it kinetically induced because under neutral and weakly acidic conditions the ligand exchange is so slow that the pH dependence disappears.

In summary, by taking advantage of the flow control and the presence of multiple electrodes in a microfluidic channel, we have implemented a principle of chemical coupling that biological systems extensively utilize to overcome the severe thermodynamic constraints in life-sustaining processes.[13] As a proof of concept, we used this principle to enhance the electrochemical sensitivity of a pH-dependent reaction and showed that is not necessary to change the pH of the whole solution to attain advantageous effects in detection. This could be beneficial in integrated bioanalysis in which the pH prior to the detection stage needs to be restricted. Furthermore, since this approach can be applied to any pair of reactions sharing a common reactant or product (including electrochemical, photonic, and chemical reactions), we are currently investigating coupling schemes that could lead to

signal amplification. Finally, the coupling can be modulated easily by simply changing the flow rate or interelectrode gap.

Experimental Section

The microfluidic cells made of poly(dimethylsiloxane) (PDMS) and gold- or indium-tin-oxide-coated glass were fabricated following photolithographic procedures.[20,21] A typical microelectrochemical cell consisted of a rectangular PDMS channel (500 μm wide and 25 μm high) glued onto the glass surface (see the Supporting Information). The patterned electrodes (200 μm wide and 150 μm apart) were located close to a big circular reservoir in which a Pt and an Ag wire were used as counter and quasi-reference electrodes, respectively. All experiments were conducted with a bipotentiostat (CH Instruments, Austin, TX) by pulsing the potential of E_2 (0.1 s) while keeping the potential of E_1 at the desired value. The uncompensated resistance was always about 20 kΩ and $E_{1/2} \approx E^{\circ\prime}$ when $D_{ox} = D_{red}$ is assumed.[22] The flow rate (1 μL min^{-1}) was controlled with a precision syringe pump (Harvard Apparatus, Holliston, MA).

Received: April 26, 2006
Published online: July 31, 2006

Keywords: electrochemistry · microfluidics · sensors · signal transduction

[1] C. Amatore, A. Oleinick, O. V. Klymenko, I. Svir, *ChemPhysChem* **2005**, *6*, 1581 – 1589.
[2] A. C. Fisher, R. G. Compton, *J. Appl. Electrochem.* **1991**, *21*, 208 – 212.
[3] M. Thompson, O. V. Klymenko, R. G. Compton, *J. Electroanal. Chem.* **2005**, *576*, 333 – 338.
[4] M. Zhong, J. Zhou, S. M. Lunte, G. Zhao, D. M. Giolando, J. R. Kirchhoff, *Anal. Chem.* **1996**, *68*, 203 – 207.
[5] I. E. Henley, K. Yunus, A. C. Fisher, *J. Phys. Chem. B* **2003**, *107*, 3878 – 3884.
[6] R. G. Compton, R. A. W. Dryfe, J. A. Alden, N. V. Rees, P. J. Dobson, P. A. Leigh, *J. Phys. Chem.* **1994**, *98*, 1270 – 1275.
[7] R. G. Compton, J. J. Gooding, A. Sokirko, *J. Appl. Electrochem.* **1996**, *26*, 463 – 469.
[8] M. E. Robbins, E. D. Hopper, M. H. Schoenfisch, *Langmuir* **2004**, *20*, 10296 – 10302.
[9] C. R. Cabrera, B. Finlayson, P. Yager, *Anal. Chem.* **2001**, *73*, 658 – 666.
[10] S. M. Mitrovski, R. G. Nuzzo, *Lab Chip* **2005**, *5*, 634 – 645.
[11] J. Pihl, J. Sinclair, E. Sahlin, M. Karlsson, F. Petterson, J. Olofsson, O. Orwar, *Anal. Chem.* **2005**, *77*, 3897 – 3903.
[12] C. A. Paddon, G. J. Pritchard, T. Thiemann, F. Marken, *Electrochem. Commun.* **2002**, *4*, 825 – 831.
[13] R. H. Garrett, C. M. Grisham, *Biochemistry*, 3rd ed., Thomson Brooks/Cole, Belmont, **2005**, p. 1086.
[14] P. Karabinas, D. Jannakoudakis, *J. Electroanal. Chem.* **1984**, *160*, 159 – 167.
[15] J. Q. Chambers in *The Chemistry of the Quinonoid Compounds*, *Vol. 2* (Eds.: S. Patai, Z. Rappoport), Wiley, New York, **1988**, pp. 719 – 757, and references therein.
[16] M. M. Walczak, D. A. Dryer, D. D. Jacobson, M. G. Foss, N. T. Flynn, *J. Chem. Educ.* **1997**, *74*, 1195 – 1197.
[17] S. Fledler, R. Hagedorn, T. Schnelle, E. Richter, B. Wagner, G. Fuhr, *Anal. Chem.* **1995**, *67*, 820 – 828.
[18] K. P. McNamara, T. Nguyen, G. Dumitrascu, J. Ji, N. Rosenzweig, Z. Rosenzweig, *Anal. Chem.* **2001**, *73*, 3240 – 3246.
[19] P. C. Ford, J. R. Kuempel, H. Taube, *Inorg. Chem.* **1968**, *7*, 1976 – 1983.
[20] Y. N. Xia, G. M. Whitesides, *Angew. Chem.* **1998**, *110*, 568 – 594; *Angew. Chem. Int. Ed.* **1998**, *37*, 550 – 575.
[21] W. Zhan, J. Alvarez, R. M. Crooks, *J. Am. Chem. Soc.* **2002**, *124*, 13265 – 13270.
[22] A. J. Bard, L. R. Faulkner, *Electrochemical Methods Fundamentals and Applications*, 2nd ed., Wiley, New York, **2001**, p. 344.

